Practical design of the optical lever intracavity topology of gravitational-wave detectors

S. L. Danilishin* and F. Ya. Khalili

Physics Faculty, Moscow State University, Moscow 119992, Russia

(Received 20 September 2005; published 19 January 2006)

The quantum nondemolition (QND) intracavity topologies of gravitational-wave detectors proposed several years ago allow us, in principle, to obtain sensitivity significantly better than the standard quantum limit using relatively small amount of optical pumping power. In this article we consider an improved more practical version of the *optical lever* intracavity scheme. It differs from the original version by the symmetry which allows to suppress influence of the input light amplitude fluctuation. In addition, it provides the means to inject optical pumping inside the scheme without increase of optical losses. We consider also sensitivity limitations imposed by the *local meter* which is the key element of the intracavity topologies. Two variants of the local meter are analyzed, which are based on the spectral variation measurement and on the discrete sampling variation measurement, correspondingly. The former one, while can not be considered as a candidate for a practical implementation, allows, in principle, to obtain the best sensitivity and thus can be considered as an ideal ''asymptotic case'' for all other schemes. The DSVM-based local meter can be considered as a realistic scheme but its sensitivity, unfortunately, is by far not so good just due to a couple of peculiar numeric factors specific for this scheme. From our point of view search of new methods of mechanical QND measurements probably based on improved DSVM scheme or which combine the local meter with the pondermotive squeezing technique, is necessary.

DOI: 10.1103/PhysRevD.73.022002 PACS numbers: 04.80.Cc, 04.30.Db

I. INTRODUCTION

The large-scale laser interferometric gravitational-wave detectors [1–4] which have been built to search gravitational waves from very distant astrophysical sources represent now the most sensitive measurement devices for mechanical acceleration and displacement. Currently their sensitivity is close to $\sqrt{S_x} = 10^{-19}$ m/Hz$^{1/2}$ in frequency range $100 \div 200$ Hz [5]. This value is only $\sim$30 times larger than the standard quantum limit (SQL) of these devices sensitivity [6–8].

The next generation of terrestrial gravitational-wave detectors probably will reach this limit in 2008–2010 [9,10], and then overcome it. The overcoming of the SQL will require more or less significant modification of the detectors topology. Several variants of this modification have been proposed. They can be divided into two groups.

The first group [11–23] (which can be considered as the ''mainstream'') preserves in general the current detector topology. We will refer to these schemes below as *extracavity* ones because all of them convert phase shift of the optical pumping field created by the gravitational-wave signal into some modulation of the output light beam which is detected by photodetector(s) *outside* the interferometer optical cavities.

Unfortunately, due to semitechnological limitations common for all these schemes [24] they can not provide sensitivity significantly better than the SQL. The second group of methods, so-called *intracavity* schemes [25–29], requires more radical modification of the detector topology but can provide substantially better sensitivity with smaller value of optical pumping power. The basic idea of this method was proposed in the article [25] and can be formulated as the following: measure directly the redistribution of optical energy created by the gravitational wave *inside* the detector in a QND way (without absorption of optical quanta).

In the article [26] a possible implementation of this idea, the *optical bars* scheme, was proposed (see Fig. 1, left). In this scheme the end mirrors E_1, E_2 and the central mirror C form two Fabry-Perot cavities coupled by means of a partly transparent mirror C. Relatively weak external optical pumping is necessary in order to compensate internal losses in the optical elements and support the steady value of optical energy circulating inside the cavities. It can be injected into the scheme through the slightly transparent auxiliary mirror D.

Such system set of eigenfrequencies represents a series of doublets, with frequencies in each doublet separated by the beating frequency

$$\Omega_B = \frac{cT_{\mathsf{C}}}{L} \tag{1}$$

(notations used in this paper are gathered in Table I). If the upper frequency mode of some of the doublets is pumped then optical field acts as two rigid springs one of which is located between the mirrors E_1 and C and the second one (L-shaped)—between the mirrors E_2 and C. This is the same optical rigidity that can exist in a single cavity [30–32] and in the signal-recycled topology of laser interferometric gravitational-wave detectors [14].

*Electronic address: stefan@hbar.phys.msu.ru
†Electronic address: farid@hbar.phys.msu.ru

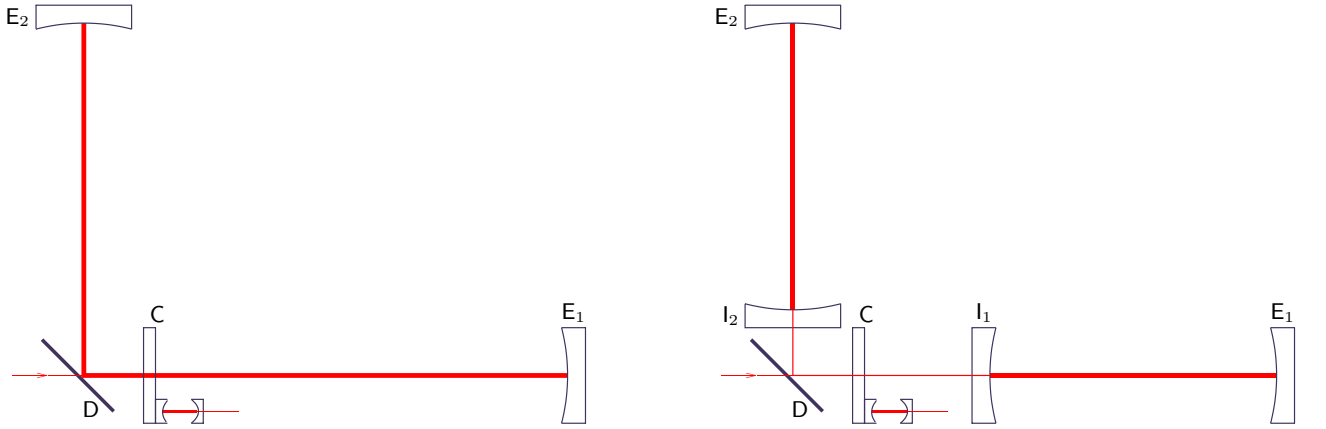

FIG. 1 (color online). The "optical bars" (left) and "optical lever" (right) intracavity schemes.

Because of these springs displacement of the end mirrors $\mathsf{E}_{1,2}$ caused by the gravitational wave produces displacement of the local mirror C. The local mirror should have an attached measurement device (*local meter*) which monitors its position relative to some reference mass placed outside the optical field.

In the article [28] an improved version of the *optical bars* scheme was proposed. It differs from the original "optical bars" scheme by two additional mirrors I_1 and I_2 (see Fig. 1, right) which turn the antenna arms into two Fabry-Perot cavities, similar to the standard Fabry-Perot—Michelson topology of the contemporary gravitational-wave antennae. In this topology,

$$\Omega_B \approx \gamma \frac{T_\mathsf{C}}{R_\mathsf{C}}. \tag{2}$$

TABLE I. Main notations used in this paper.

Quantity	Value	Description
A	$\sqrt{3\times10^{-5}}$	Arm cavities amplitude loss per bounce
A_{local}	$\sqrt{5\times10^{-6}}$	Local meter cavity amplitude loss per bounce
c		Speed of light
$\mathcal{F}$		Arm cavities finesse
$\mathsf{F}\approx\frac{2}{\pi}\mathcal{F}$		Signal displacement gain
$\hbar$		Plank's constant
L	4 km	Arm cavities length
l		Local meter cavity length
M_C		Central mirror mass
M_E		End mirrors mass
M_I		Input mirrors mass
$M=\frac{2M_\mathsf{E}M_\mathsf{I}}{M_\mathsf{E}+M_\mathsf{I}}$	40 kg	
$\mu=M/\mu^2$		
$m_+=M_\mathsf{C}+\mu$		Equivalent sum mass of the system
$m_*=\frac{\mu M_\mathsf{C}}{\mu+M_\mathsf{C}}$		Equivalent reduced mass of the system
$R_\mathsf{C}, T_\mathsf{C}$		Central input mirror amplitude reflectivity and transmittance
T_{local}		Local meter input mirror amplitude transmittance
W		Optical power circulating in the arm cavities
w		Optical power circulating in local meter cavity
γ		Arm cavities half-bandwidth
$\gamma_{\mathrm{loss}}=\frac{cA^2}{4L}$	$0.6\ \mathrm{s}^{-1}$	Part of γ caused by the optical losses
ω_o	$1.8\times10^{15}\ \mathrm{s}^{-1}$	Optical pumping frequency
Ω	$2\pi\times100\ \mathrm{s}^{-1}$	Signal (side-band) frequency
Ω_B		Beating frequency
Ω_0		Mechanical resonance frequency
τ		DSVM sampling time

This scheme was called *optical lever* because it can provide the gain in signal displacement of the local mirror similar to the gain which can be obtained using ordinary mechanical lever with unequal arms. The value of this gain is equal to

$$F \approx \frac{c}{\gamma L} = \frac{2}{\pi}\mathcal{F}. \tag{3}$$

In the article [28] it was shown that in all other aspects the *optical lever* scheme is identical to the *optical bars* one, but in the former one the local mirror C mass has to be F^2 times smaller. Because of this scaling of mass the gain in signal displacement by itself does not allow to overcome the SQL, because the SQL value increases exactly in the same proportion. But it allows to use less sensitive local position meter (thus decreasing substantially required optical power in it) and increases the signal-to-noise ratio for miscellaneous noises of nonquantum origin.

In the article [29] prospects of use of QND local meter (mentioned first briefly in the article [27]) were analyzed. It was shown that QND local meter allows to decrease significantly the optical power circulating in the main cavity, while providing sensitivity several times better than the standard quantum limit.

The main goal of the current paper is further development of the *optical lever* topology towards practical design of the intracavity gravitational-wave detector. In particular, we consider its integration with the local meter based on the discrete sampling variation measurement (DSVM) procedure [33].

This paper is organized as the following.

In the Sec. II we discuss the semitechnological limitations mentioned above and estimate sensitivities which can be provided by extracavity and intracavity topologies.

In the Sec. III A modified topology of the *optical lever* scheme which can be considered as more ''practical'' one is proposed. It differs from the previous one by its symmetry, which allows to suppress influence of the input light amplitude fluctuation. In addition, it provides the means to inject optical pumping inside the scheme without increase of the signal mode coupling with the external world (i.e. without increase of the optical losses).

In the Sec. III B scheme potential sensitivity, i.e. the sensitivity limitation imposed by the optical losses, is analyzed. In the previous papers [27,29] this limitation was estimated only for the simplified model based on two harmonic oscillators. Now we calculate it accurately.

In the Sec. IV possible implementation of the local meter, which is evidently the key element of the intracavity topologies, is analyzed in detail. We consider in this section the combination of the optical lever topology with the DSVM scheme [33] and calculate its sensitivity.

II. INTRACAVITY VS. EXTRACAVITY TOPOLOGIES

A. Optical power

It is well known that in order to detect tiny gravitational-wave signal huge amount of optical quanta is required. Usual explanation of this requirement is the following. In the interferometric gravitational-wave detectors the phase of the optical field is monitored. Precision of this measurement is limited by the phase quantum fluctuations (i.e. the shot noise) which spectral density is inversely proportional to the mean optical power.

In the QND modifications of the standard topology, for example, variational input/output schemes [8,16,17], not phase but some combination of the phase and amplitude quadratures of the optical field is monitored. In this case more general explanation [24] based on the Heisenberg uncertainty relation can be provided.

Really, in order to detect displacement $\sim Lh$ of the end mirrors created by the gravitational wave it is necessary to provide perturbation of its momentum $\Delta p \geq \hbar/2\delta x$. The only source of this perturbation in the interferometric gravitational-wave antennae is the uncertainty of the optical pumping energy: $\Delta p \propto \Delta\mathcal{E} = \langle\mathcal{E}\rangle/\zeta^2$, where $\zeta = e^{-R}$ is the squeeze factor and $\langle\mathcal{E}\rangle$ is the mean energy. Therefore, the smaller δx has to be detected, the higher energy is required.

In spectral representation uncertainty relation for the interferometric gravitational-wave detectors can be presented as the following[1]:

$$\frac{L^2 S_h}{4} \times S_{\text{B.A.}} = \frac{\hbar^2}{4}, \tag{4}$$

where S_h is the spectral density of the measurement noise, normalized as fluctuation metrics variation, and $S_{\text{B.A.}}$ is the spectral density of the fluctuation radiation pressure differential force acting on each of the test mirrors.

It is evident that for all extracavity topologies $S_{\text{B.A.}} \propto W/\zeta^2$. Exact form of this spectral density depends on the specific topology. For the ordinary Initial LIGO topology

$$S_{\text{B.A.}} = \frac{8\hbar\omega_p W}{\zeta^2 cL}\frac{\gamma}{\gamma^2+\Omega^2}, \tag{5}$$

and therefore

$$S_h = \frac{\zeta^2\hbar c}{8L\omega_p W}\frac{\gamma^2+\Omega^2}{\gamma}. \tag{6}$$

It is convenient to compare this spectral density with the one corresponding to the standard quantum limit:

[1]In this article, we use ''two-sided'' spectral densities which 2 times smaller than ''one-sided'' ones and provide a bit more consistent formulae.

$$\xi^2_{\rm extra} \equiv \frac{S_h}{S_h^{\rm SQL}} = \frac{\zeta^2}{2}\frac{W_{\rm SQL}}{W}\frac{\gamma^2+\Omega^2}{2\gamma\Omega}, \tag{7}$$

where

$$S_h^{\rm SQL} = \frac{4\hbar}{M\Omega^2L^2} \tag{8}$$

(see [8]), and

$$W_{\rm SQL} = \frac{McL\Omega^3}{8\omega_o} \tag{9}$$

is the circulating optical power in the SQL-limited detector which is necessary to reach the SQL. Factor $1/2$ corresponds to the evident fact that QND techniques provide $\sqrt{2}$ times better sensitivity than SQL-limited detector even if $W = W_{\rm SQL}$, because they "filter out" backaction noise which for $W = W_{\rm SQL}$ corresponds to one half of the total noise.

In the *speed-meter* topologies [18–23] $S_{\rm B.A.}$ differs only by an additional factor $2\Omega^2/(\gamma^2+\Omega^2)$. Therefore, if $\Omega \simeq \gamma$ then sensitivity is close to 1 defined by Eq. (6).

On the other hand, in the signal-recycled "optical springs" topology [12–17] it is possible to create high narrow peak in spectral dependence of $S_{\rm B.A.}$:

$$S_{\rm B.A.} = \frac{4\hbar\omega_p W}{\zeta^2 cL}\frac{\Delta\Omega/2}{(\Omega-\Omega_0)^2+(\Delta\Omega/2)^2}. \tag{10}$$

The peak width $\Delta\Omega$ and the mean frequency Ω_0 depend on the signal recycling mirror cavity parameters. Therefore, in this case it is possible to obtain sensitivity much better than the SQL without increase of optical power, but only in narrow spectral band $\Delta\Omega \ll \Omega_0$:

$$\xi^2_{\rm extra} = \frac{\zeta^2}{2}\frac{W_{\rm SQL}}{W}\frac{(\Omega-\Omega_0)^2+(\Delta\Omega/2)^2}{\Omega_0\Delta\Omega/2}, \tag{11}$$

$$\xi^2_{\rm extra}\Big|_{\Omega=\Omega_0} = \frac{\zeta^2}{2}\frac{W_{\rm SQL}}{W}\frac{\Delta\Omega/2}{\Omega_0}. \tag{12}$$

Below we limit ourselves to the wide-band case (7) only.

B. Optical losses

It follows from Eq. (7) that the best sensitivity can be achieved if $\gamma \simeq \Omega$, and at this point

$$\xi^2_{\rm meter} = \frac{\zeta^2}{2}\frac{W_{\rm SQL}}{W}. \tag{13}$$

Unfortunately, situation is possible where this optimization can not be provided. Really, it can be shown that internal losses in the optical elements impose the following additional limitation on the sensitivity:

$$\xi^2_{\rm loss} = \sqrt{\zeta^2\frac{\gamma_{\rm loss}}{\gamma_{\rm load}}} \approx \sqrt{\zeta^2\frac{\gamma_{\rm loss}}{\gamma}}. \tag{14}$$

Suppose that $\gamma \approx \Omega$. In this case sensitivity will be limited by the following value:

$$\xi^2_{\rm loss} \approx \sqrt{\zeta^2\frac{\gamma_{\rm loss}}{\Omega}}. \tag{15}$$

For the Advanced LIGO values of parameters (see Table I),

$$\gamma_{\rm loss} = \frac{cA^2}{4L} \simeq 0.6\ {\rm s}^{-1}, \tag{16}$$

and

$$\xi_{\rm loss} \approx 0.2\sqrt{\zeta}. \tag{17}$$

In order to obtain smaller $\xi_{\rm loss}$ it is necessary to increase γ thus increasing $\xi_{\rm meter}$. It is evident that the optimal value of γ exists, which provides minimum to the sum noise spectral density:

$$\xi^2_{\rm sum} = \xi^2_{\rm extra} + \xi^2_{\rm loss} \approx \frac{\zeta^2}{2}\frac{W_{\rm SQL}}{W}\frac{\gamma}{2\Omega} + \sqrt{\zeta^2\frac{\gamma_{\rm loss}}{\gamma}} \tag{18}$$

(it is supposed here for simplicity that $\gamma \gg \gamma_{\rm loss}$, $\gamma \gg \Omega$). The minimum is reached when

$$\gamma = \left(\frac{4\gamma_{\rm loss}\Omega^2}{\zeta^2}\frac{W^2}{W_{\rm SQL}^2}\right)^{1/3}, \tag{19}$$

and is equal to:

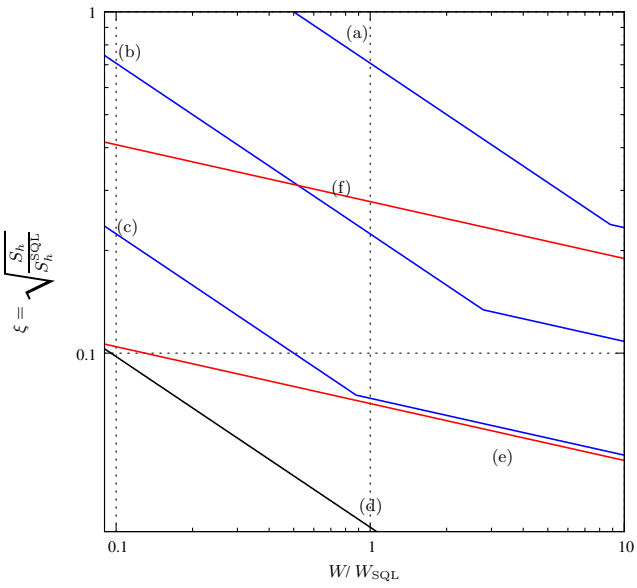

FIG. 2 (color online). (a): Sensitivity which can be obtained in the standard extracavity topology for the coherent pumping; (b): the same for the 10 dB squeezed pumping; (c): 20 dB squeezed pumping. The left more steep parts of curves (a)–(c) correspond to Eq. (7) with $\gamma = \Omega$, the right more flat ones—to Eq. (20). (d): Potential sensitivity of the intracavity optical lever topology; (e) sensitivity of the optical lever scheme with the spectral variation measurement-based local meter; (f) sensitivity of the optical lever scheme with the DSVM-based local meter.

$$\xi_{\rm sum}^2 = \frac{3}{2}\left(\zeta^4 \frac{\gamma_{\rm loss}}{2\Omega}\frac{W_{\rm SQL}}{W}\right)^{1/3}. \quad (20)$$

For the values of $\gamma_{\rm loss}$ and Ω mentioned above we obtain that

$$\xi_{\rm sum} \approx 0.34 \times \zeta^{2/3} \times \left(\frac{W_{\rm SQL}}{W}\right)^{1/6}. \quad (21)$$

Note the very weak dependence on pumping power.

The sensitivity estimates based on Eqs. (7) and (20) are plotted in Fig. 2 as functions of optical power, see curves (a),(b),(c).

III. PRACTICAL VERSION OF THE *OPTICAL LEVER* INTRACAVITY TOPOLOGY

A. Discussion of the topology

The scheme which is analyzed in this paper is presented in Fig. 3. Consider step by step the additional optical elements of this scheme.

1. Symmetrization of the topology

The evident disadvantage of simple schemes shown in Fig. 1 is their nonsymmetry: pumping power enters the ''north'' (vertical on the picture) arm first and only then, through the coupling mirror C, the ''east'' one. Because of this nonsymmetry the input optical field amplitude fluctuations will create differential pondermotive force acting on the central mirror and imitating gravitational-wave signal. In order to eliminate this effect, symmetric power injection scheme shown in Fig. 3 has to be used. It consists of the beamsplitter BS which splits the input beam into two, and two additional power injection mirrors D_1 and D_2 placed symmetrically on both sides of the central mirror C.

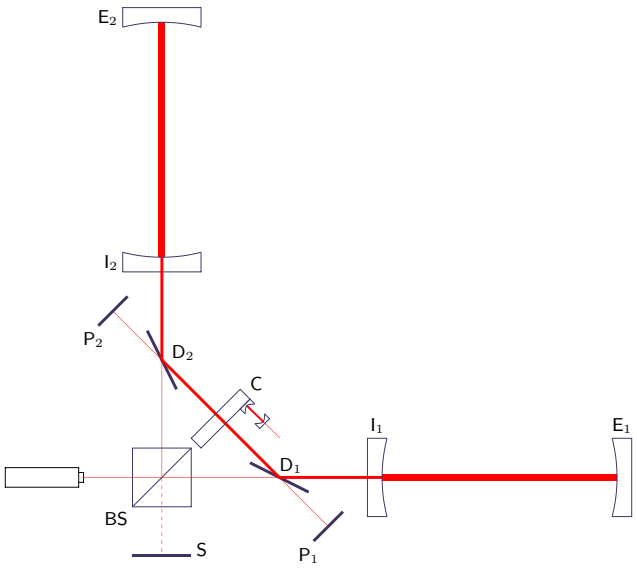

FIG. 3 (color online). Practical design of the *optical lever* intracavity scheme.

2. Power recycling mirrors

It can be shown that without power recycling mirrors P_1, P_2 one quarter of input power is reflected from the mirrors D_1 and D_2 back to the laser, another quarter is reflected to the side direction, and only one half enters the scheme. The mirrors P_1, P_2 cancel both reflected beams and increase twice the circulating power inside the scheme (for the same value of input power).

3. Signal recycling mirror

It can be shown also that if the mirrors $\mathsf{D}_{1,2}$ transmittances are tuned in optimal way to provide maximal optical power in the scheme [see Eq. (A9)] then these transmittances will create an additional ''hole'' which will increase two-fold total optical losses in the scheme.

This hole can be closed without affecting optimal coupling condition using symmetry of the scheme. Indeed, similar to traditional interferometric gravitational-wave detectors topology, the mean value of optical power inside the scheme depends on the bandwidth of the symmetric optical mode which is coupled with ''western'' port of the beamsplitter, and the detector sensitivity depends on the bandwidth of antisymmetric mode which is coupled with ''south'' port of the beamsplitter. The only difference is that in traditional topology the antisymmetric mode bandwidth has to be close to the signal frequency Ω to provide optimal coupling with photodetector, while in the intracavity topology it has to be as small as possible. Therefore, high-reflectivity signal recycling mirror has to be placed in the south port as shown in Fig. 3.

B. Sensitivity limitation due to optical losses

The topology described in the previous subsection is analyzed in the Appendix A. In particular, the sensitivity limitation imposed by optical losses is calculated. Spectral density of the corresponding equivalent noise (normalized as fluctuation metrics variation) is equal to

$$S_h^{\rm loss} \approx \frac{\hbar c \gamma_{\rm loss}}{2\omega_o W L}\left(1 + \frac{\Omega^2}{\Omega_B^2}\right). \quad (22)$$

(slightly simplified form is presented here, which takes into account that $\Omega_B \geq \Omega \gg \gamma_{\rm loss}$; for the exact form, see Eq. (A44)).

Compare this spectral density with the one corresponding to the Standard Quantum Limit [see Eqs. (8) and (9)]:

$$\xi_{\rm loss}^2 \equiv \frac{S_{h\rm loss}}{S_h^{\rm SQL}} = \frac{\gamma_{\rm loss}}{\Omega}\frac{W_{\rm SQL}}{W}\left(1 + \frac{\Omega^2}{\Omega_B^2}\right). \quad (23)$$

It was noted in the article [29] that due to the fact that factor $\gamma_{\rm loss}/\Omega$ can be as small as $\sim 10^{-3}$, the value $\xi_{\rm loss} \ll 1$ can be obtained even with $W \ll W_{\rm SQL}$.

Estimate of $\xi_{\rm loss}$ as a function of $W/W_{\rm SQL}$ (the potential sensitivity) is plotted in Fig. 2, see curve (d).

IV. LOCAL METER

A. Options for the local meter

Taking into account the gain $F \sim 10 \div 100$ in the local mirror mechanical displacement, sensitivity of the local meter has to be several times better than SQL for the mass $\mu = M/F^2$:

$$\sqrt{\frac{\hbar}{\mu\Omega^2}} = F\sqrt{\frac{\hbar}{M\Omega^2}} \sim (10 \div 100) \times 2.5 \times 10^{-19}\,\mathrm{m} \times \mathrm{s}^{-1/2}. \tag{24}$$

Several types of devices have been proposed, which can, in principle, provide this sensitivity, in particular: SQUID-based schemes used in solid-state gravitational-wave antennae; microwave speed meter [18]; small-scale optical speed meter [21]; spectral variation measurement-based schemes (a.k.a. schemes with modified input-output optics) [11,17]; and the discrete sampling variation measurement (DSVM) based optical position meter [33].

The first two types require cryogenic equipment. In addition, estimates made in the article [18] show that due to the internal losses the microwave spped meter can provide sensitivity only slightly better than SQL.

The Sagnac-based optical spped meter (as well as other practical speed-meter schemes) requires that its optical storage time has to be larger than $\Omega^{-1} \sim 10^{-3}$ s. Simple estimates show that due to this limitation the interferometer size can not be smaller than $\sim$100 m, i.e. an additional setup comparable with a full scale gravitational-wave detector, such as GEO-600, is necessary.

In spectral variation measurement-based (variational input/output) schemes a short (desktop-scale) main cavity can be used. However, they require an additional cavity with bandwidth comparable with the signal frequency and thus with hundreds meters length.

We consider here two variants of the local meter: the spectral variation measurement-based and DSVM-based schemes. The former one, while it can not be considered as a candidate for a practical implementation, allows, in principle, to obtain the best sensitivity and thus can be considered as an ideal ''asymptotic case'' for all other schemes. The DSVM-based local meter can be considered as a realistic scheme but its sensitivity, unfortunately, is by far not so good just due to a couple of peculiar numeric factors specific for this scheme.

Both these schemes use Fabry-Perot cavity-based position meter with a homodyne detector. The evident technical challenge in this case is how to attach this meter to the small (with the mass of about 1 g) local mirror which is also the part of the main large-scale optical setup. Possible solution which is based on the scheme proposed in the paper [34] is shown in Fig. 4.

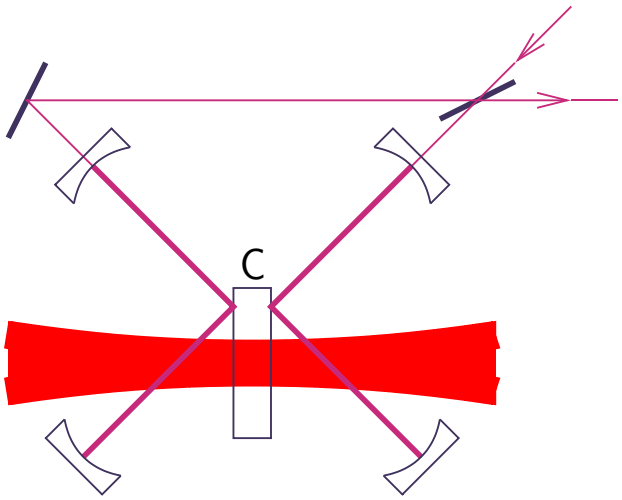

FIG. 4 (color online). Possible design of local meter.

B. Ideal variation measurement

Suppose that the local oscillator phase $\phi_{\rm LO}$ of the homodyne detector mentioned above can depend on the observation frequency Ω in an arbitrary way. It was shown in the article [11] that by special tuning of the function $\phi_{\rm LO}(\Omega)$ it is possible to eliminate the backaction noise from the output signal and thus to overcome the SQL.

Spectral density of this scheme measurement noise is calculated in Appendix , see Eq. (B7). It follows from this equation that the sensitivity limitation imposed by the meter can be presented as follows:

$$\xi^2_{\rm meter} \equiv \frac{S_h^{\rm meter}}{S_h^{\rm SQL}} = \frac{\mathcal{I}}{2}\,\frac{m_+^2}{\mu M_{\rm C}}\,\frac{w_{\rm SQL}}{w}, \tag{25}$$

where

$$\mathcal{I} = \frac{[\Omega^4 - \Omega^2\Omega_B^2 + \Omega_0^2\Omega_B^2]^2}{\Omega_0^4\Omega_B^4}, \tag{26}$$

and

$$w_{\rm SQL} = \frac{M_{\rm C}c^2T_{\rm local}^2\Omega^2}{32\omega_o} \tag{27}$$

is circulating power in an ordinary (SQL-limited) Fabry-Perot cavity-based position meter which is necessary to reach the SQL for the test mass $M_{\rm C}$.

Factor $\mathcal{I}$ has rather sophisticated spectral dependence. It is evident, however, that the best sensitivity area corresponds to values $\Omega \sim \Omega_0 \sim \Omega_B$, and the noise spectral density increases as Ω^4 if $\Omega \gg \Omega_B \sim \Omega_0$.

We consider here simple particular case when

$$\Omega \le \Omega_B = 2\sqrt{2}\Omega_0. \tag{28}$$

(for more general optimization, see Appendix C of the

article [29]). In this case $\mathcal{I} \leq 1$. On the other hand, condition (29) together with Eq. (A47) lead to the following limitation on the pumping power W:

$$W \geq \frac{\mathcal{F}^2 m_* c L \Omega^3}{64\omega_o} = \frac{1}{8}\frac{m_*}{\mu} W_{\mathrm{SQL}}. \tag{29}$$

It was pointed in the article [29] that it is possible to reduce pumping power by using small local mirror with mass $M_{\mathrm{C}} \ll \mu$. In this case,

$$m_+ \approx \mu, \qquad m_* \approx M_{\mathrm{C}}, \tag{30}$$

and Eqs. (26) and (30), can be simplified:

$$\xi^2_{\mathrm{meter}} = \frac{\mathcal{I}}{2\mathcal{F}^2}\frac{M}{M_{\mathrm{C}}}\frac{w_{\mathrm{SQL}}}{w}, \tag{31a}$$

$$W \geq \frac{\mathcal{F}^2}{8}\frac{M_{\mathrm{C}}}{M} W_{\mathrm{SQL}}, \tag{31b}$$

The meaning of these equations is evident. The larger is $\mathcal{F}$, the better is sensitivity because the local mirror signal displacement is proportional to $\mathcal{F}$. On the other hand, the larger is $\boldsymbol{\mathcal{F}}$, the larger has to be circulating power in the arm cavities to keep optical springs sufficiently stiff. Excluding factor $\mathcal{F}$ Eqs. (31) can be combined into the following one:

$$\xi^2_{\mathrm{meter}} = \frac{1}{16}\frac{W_{\mathrm{SQL}}}{W}\frac{w_{\mathrm{SQL}}}{w}. \tag{32}$$

In Eq. (32) optical losses in the local meter cavity have not been taken into account. These losses impose an additional sensitivity limitation which has the same form as condition (14):

$$\xi^2_{\mathrm{loss}} = \sqrt{\frac{A^2_{\mathrm{local}}}{T^2_{\mathrm{local}}}}. \tag{33}$$

The smaller is T_{local}, the smaller is ξ_{meter}, but the larger is ξ_{loss}. Therefore, an optimal value of T_{local} exists where the sum

$$\xi^2_{\mathrm{meter\,loss}} = \xi^2_{\mathrm{meter}} + \xi^2_{\mathrm{loss}} \tag{34}$$

is minimum. It is easy to show that at this point,

$$\xi^2_{\mathrm{meter\,loss}} = \frac{\xi^2_0}{2}\left(\frac{W_{\mathrm{SQL}}}{W}\right)^{1/3}, \tag{35}$$

where

$$\xi^2_0 = \frac{3}{2}\left(\frac{M_{\mathrm{C}} c^2 A^2_{\mathrm{local}}\Omega^2}{32\omega_o w}\right)^{1/3}. \tag{36}$$

For numeric estimates, we will use the same values as proposed for the pondermotive squeezing experiment in [34], see Table I. For these values $\xi_0 \approx 0.1$ thus allowing to obtain for the optical power $W \lesssim W_{\mathrm{SQL}}$ the value of $\xi_{\mathrm{meterloss}}$ which is also close to 0.1. Graphs of $\xi_{\mathrm{meter\,loss}}$ as a function of W are plotted in Fig. 2, see curve (e).

C. DSVM-based local meter

The scheme of the DSVM-based local meter, similar to the previous one, consists of a Fabry-Perot cavity-based position meter with a homodyne detector. However, instead of the frequency-dependent local oscillator phase time-dependent one is used in order to exclude the back-action noise.

This method is based on variation measurement technique proposed in [35] and analyzed in [36,37]. Severe disadvantage of this original form of variation measurement is the necessity to know the shape and arrival time of the signal being detected. DSVM procedure suggests the way to overcome this disadvantage by approximating the real signal with the sequence of rectangular pulses which amplitude is the mean value of the signal over the pulse duration $\tau \leq \pi/\Omega_{\max}$, where $\Omega_{\max}$ is the upper frequency of the signal.

Sensitivity of the DSVM-based local meter is calculated in Appendix B 2. It is shown that if this meter is used then

$$\xi^2_{\mathrm{DSVM}} \equiv \frac{S_h^{\mathrm{meter}}}{S_h^{\mathrm{SQL}}} = \frac{720}{\pi^4 \mathcal{G}(\Omega_B\tau, \Omega_0\tau)}\frac{m_+^2}{\mu M_{\mathrm{C}}}\frac{w_{\mathrm{SQL}}}{w} \tag{37}$$

(it is supposed here that $\Omega = \Omega_{\max}$).

Dimensionless function $\mathcal{G}(\Omega_B\tau, \Omega_0\tau)$ is calculated numerically and its 3D-plot is presented in Fig. 5. Three areas can be clearly distinguished on this plot depending on the mechanical eigenfrequency Ω_0 and beating frequency Ω_B.

1. $\Omega_0 > \Omega_B/2$. In this area the system is extremely unstable: its eigenfrequencies have imaginary parts of both signs comparable with the real ones. We expressed symbolically this instability by setting $\mathcal{G} = 0$ (i.e. $S_h^{\mathrm{meter}} \to \infty$) in this area.

2. $\Omega_B/2 > \Omega_0 \gtrsim 3\Omega_{\max}$. In this area, $\mathcal{G}$ is close to its maximum value 1 and therefore the best sensitivity is provided. Condition $\Omega_0 \gtrsim 3\Omega_{\max}$ describes sufficiently stiff optical springs that provide the local mirror signal displacement equal to the end mirrors displacement multiplied by factor $\mathcal{F}$.

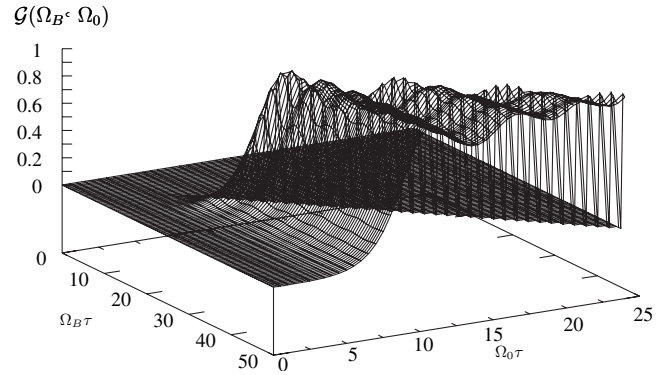

FIG. 5. 3D plot of function $\mathcal{G}(\Omega_B\tau, \Omega_0\tau)$.

3. $\Omega_0 \lesssim 3\Omega_{\max}$. In this area optical springs are too weak to move local mirror effectively. In this case the local mirror displacement is proportional to the rigidity Ω_0^2 and the noise spectral density (B20) to Ω_0^{-4}, correspondingly.

Below we consider the best sensitivity case where the condition

$$\Omega_B/2 > \Omega_0 \gtrsim 3\Omega_{\max} \tag{38}$$

is fulfilled and thus

$$\xi^2_{\mathrm{DSVM}} \approx \frac{720}{\pi^4}\,\frac{m_+^2}{\mu M_{\mathsf{C}}}\,\frac{w_{\mathrm{SQL}}}{w}. \tag{39}$$

On the other hand, condition (38) together with Eq. (A47) lead to the limitation on the pumping power W:

$$W \gtrsim 2\times 3^3 \times \frac{\mathcal{F}^2 m_* c L \Omega^3}{8\omega_o} \approx 60\,\frac{m_*}{\mu}\,W_{\mathrm{SQL}}. \tag{40}$$

Note that Eqs. (39) and (40) have exactly the same structure as Eqs. (25) and (29) for the ideal meter case and differ by numerical factors only. Therefore, the next consideration follows the previous subsection.

We suppose again that $M_{\mathsf{C}} \ll \mu$ and thus obtain that:

$$\xi^2_{\mathrm{DSVM}} \approx \frac{720}{\pi^4 \mathcal{F}^2}\,\frac{M}{M_{\mathsf{C}}}\,\frac{w_{\mathrm{SQL}}}{w}, \tag{41a}$$

$$W \approx 60\mathcal{F}^2\,\frac{M_{\mathsf{C}}}{M}\,W_{\mathrm{SQL}}. \tag{41b}$$

Combining again these two equation we obtain the following formula for the DSVM-based local meter:

$$\xi^2_{\mathrm{DSVM}} \approx \frac{720\times 60}{\pi^4}\,\frac{W_{\mathrm{SQL}}}{W}\,\frac{w_{\mathrm{SQL}}}{w}. \tag{42}$$

The final step is again optimization of T_{local} which gives that:

$$\xi^2_{\mathrm{DSVM\,loss}} \approx \xi_0^2\left(\frac{720\times 60}{\pi^4}\,\frac{W_{\mathrm{SQL}}}{W}\right)^{1/3}, \tag{46}$$

Graphs of ξ_{DSVMloss} as a function of W are also plotted in Fig. 2, see curve (f).

V. CONCLUSION

Comparing traditional extracavity topologies and intracavity topologies discussed in this article, one can conclude that the possibility to obtain sensitivity substantially better than the standard quantum limit in both cases depends in a crucial way on additional ''supporting'' device: squeezed state generator for traditional topologies, and the local meter for intracavity ones.

In both cases the best design of the supporting device, from the contemporary point of view, is based on small-scale Fabry-Perot cavity, with approximately the same requirements for the parameters.

However, intracavity topologies promise significantly better sensitivity, especially for the relatively small values of pumping power: $W < W_{\mathrm{SQL}}$. Unfortunately, none of the mechanical QND schemes known today which can be considered as practical ones, can fully realize this high potential sensitivity of intracavity topologies. From the authors point of view the search of new methods of mechanical QND measurements probably based on improved DSVM scheme or which combine the local meter with the pondermotive squeezing technique, is necessary.

ACKNOWLEDGMENTS

This work was supported in part by NSF and Caltech Grant No. PHY-0353775, by Russian Agency of Industry and Science Contracts No. 40.02.1.1.1.1137 and No. 40.700.12.0086, and by Russian Foundation for Basic Research Grant No. 03-02-16975-a.

APPENDIX A: DERIVATION OF THE MECHANICAL EQUATIONS OF MOTION

1. Notations and approximations

Additional notations used in this Appendix and not listed in Table I are gathered in Table II. Note that the optical distances between the beamsplitter and the mirror P_1, and between the beamsplitter and the mirror P_2 differ by a quarter of wave length, exactly as in the standard LIGO topology.

The following suppositions and approximation will be used:

(a) The optical ω_o pumping frequency is much larger than all other characteristic frequencies of the system.

(b) The arm cavities are tuned in resonance: $e^{2i\omega_o L/c} = 1$.

(c) The ''central station'' size is sufficiently small and it is possible to neglect the values of the order of $\frac{\Omega l_{\mathsf{D-I}}}{c}$, $\frac{\Omega l_{\mathsf{C-D}}}{c}$, $\frac{\Omega l_{\mathsf{D-P}}}{c}$, and $\frac{\Omega l_{\mathsf{BS-P}}}{c}$.

(d) All optical losses are concentrated in the arm cavities. This assumption is reasonable because losses in arm cavities appear in the final expressions amplified by the cavities finesse factor.

(e) We neglect the recycling mirrors P, S transmittances: $T_{\mathsf{S}} = T_{\mathsf{P}} = 0$ because they appear in the final expressions reduced by the mirrors $\mathcal{D}$ transmittance T_{P}.

(f) Analyzing the power (symmetric) and the signal (antisymmetric) modes we will keep first nonvanishing terms for each mode: classical (zeroth-order) field amplitudes for the power mode and linear in the mirror displacements and in the fields quantum fluctuations (i.e. first-order) terms for the signal one.

TABLE II. Some additional notations not listed in Table I.

Quantity	Description
$a_{1,2} - j_{1,2}$	Field amplitudes, see Fig. 6 (Roman letters are used)
$A_{1,2} - J_{1,2}$	Corresponding mean (classical) values (capital Roman letters are used)
$n_{1,2}$	Noises created by optical losses
R_E, R_I, *etc*	Amplitude reflectivities of the mirrors
T_E, T_I, *etc*	Amplitude transmittances of the mirrors
l_{C-D}, l_{D-I}, etc.	Optical distances between the corresponding optical elements

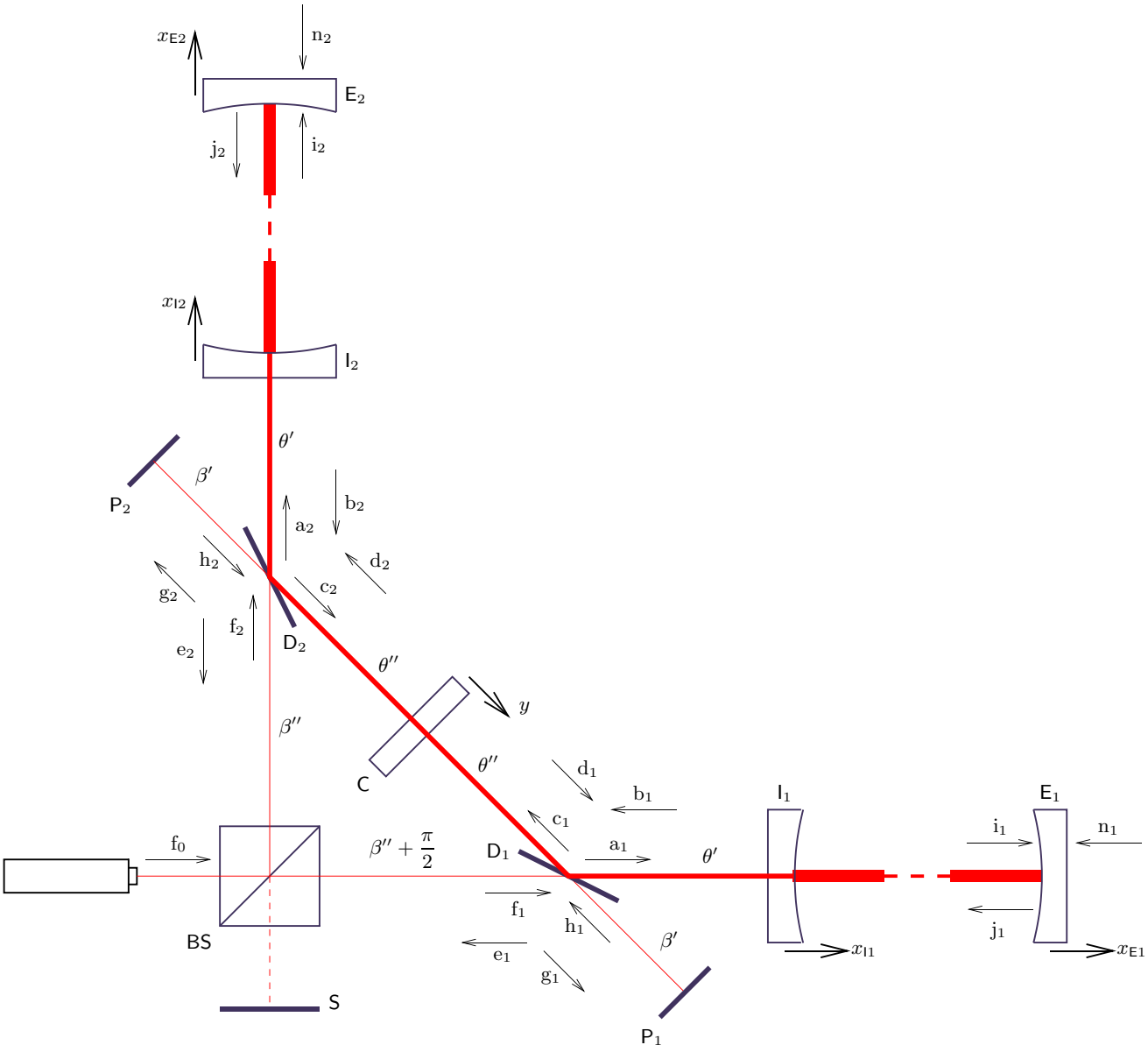

FIG. 6 (color online). The scheme.

2. Power mode

Zeroth approximation equations for the field amplitudes are the following:

$$\mathrm{A}_{1,2} = -R_{\mathsf{D}}\mathrm{D}_{1,2} + iT_{\mathsf{D}}\mathrm{F}_{1,2}, \tag{A1a}$$
$$\mathrm{B}_{1,2} = R_{\mathsf{FP}}(0)A_{1,2}e^{2i\theta'}, \tag{A1b}$$
$$\mathrm{C}_{1,2} = -R_{\mathsf{D}}\mathrm{B}_{1,2} + iT_{\mathsf{D}}\mathrm{H}_{1,2}, \tag{A1c}$$
$$\mathrm{D}_{1,2} = (-R_{\mathsf{C}}\mathrm{C}_{1,2} + iT_{\mathsf{C}}\mathrm{C}_{2,1})e^{2i\theta''}, \tag{A1d}$$
$$\mathrm{E}_{1,2} = -R_{\mathsf{D}}\mathrm{H}_{1,2} + iT_{\mathsf{D}}\mathrm{B}_{1,2}, \tag{A1e}$$
$$\mathrm{F}_{1,2} = \pm\frac{\mathrm{E}_1 - \mathrm{E}_2}{2}e^{2i\beta''} + \frac{\mathrm{F}_0}{\sqrt{2}}, \tag{A1f}$$
$$\mathrm{G}_{1,2} = -R_{\mathsf{D}}\mathrm{F}_{1,2} + iT_{\mathsf{D}}\mathrm{D}_{1,2}, \tag{A1g}$$
$$\mathrm{H}_{1,2} = -\mathrm{G}_{1,2}e^{2i\beta'}, \tag{A1h}$$
$$\mathrm{I}_{1,2} = \frac{i\sqrt{c\gamma_{\mathrm{load}}/L}}{\gamma}\mathrm{A}_{1,2}e^{i\theta'}, \tag{A1i}$$

where F_0 is the input pumping wave amplitude,

$$R_{\mathsf{FP}}(0) = \frac{\gamma_-}{\gamma} \tag{A2a}$$

is the arm cavities reflection factor at resonance frequency,

$$\gamma = \gamma_{\mathrm{load}} + \gamma_{\mathrm{loss}}, \tag{A2b}$$
$$\gamma_- = \gamma_{\mathrm{load}} - \gamma_{\mathrm{loss}}, \tag{A2c}$$
$$\gamma_{\mathrm{load}} = \frac{cT_{\mathrm{I}}^2}{4L}, \tag{A2d}$$
$$\gamma_{\mathrm{loss}} = \frac{cA^2}{4L}, \tag{A2e}$$

For Eqs. (A1b) and (A1i), see papers [22,23].

Introduce the symmetric mode (it is easy to see that the antisymmetric mode is not pumped):

$$\mathrm{A} = \frac{\mathrm{A}_1 + \mathrm{A}_2}{\sqrt{2}}, \tag{A3}$$

and correspondingly for all other fields amplitudes. Equations for these amplitudes are the following:

$$\mathrm{A} = -R_{\mathsf{D}}\mathrm{D} + iT_{\mathsf{D}}\mathrm{F}, \tag{A4a}$$
$$\mathrm{B} = R_{\mathsf{FP}}(0)\mathrm{A}e^{2i\theta'}, \tag{A4b}$$
$$\mathrm{C} = -R_{\mathsf{D}}\mathrm{B} + iT_{\mathsf{D}}\mathrm{H}, \tag{A4c}$$
$$\mathrm{D} = -\mathrm{C}e^{i(2\theta''-\phi)}, \tag{A4d}$$
$$\mathrm{E} = -R_{\mathsf{D}}\mathrm{H} + iT_{\mathsf{D}}\mathrm{B}, \tag{A4e}$$
$$\mathrm{F} = \mathrm{F}_0, \tag{A4f}$$
$$\mathrm{G} = -R_{\mathsf{D}}\mathrm{F} + iT_{\mathsf{D}}\mathrm{D}, \tag{A4g}$$
$$\mathrm{H} = -\mathrm{G}e^{2i\beta'}, \tag{A4h}$$
$$\mathrm{I} = \frac{i\sqrt{c\gamma_{\mathrm{load}}/L}}{\gamma}\mathrm{A}e^{i\theta'}, \tag{A4i}$$

where

$$\phi = \arctan\frac{T_{\mathsf{C}}}{R_{\mathsf{C}}}. \tag{A5}$$

The solution of these equations is the following (only those amplitudes which will be required later are presented):

$$\mathrm{A} = \frac{iT_{\mathsf{D}}}{\mathrm{Det}}[1 + e^{i(2\beta'+2\theta''-\phi)}]\mathrm{F}_0, \tag{A6a}$$

$$\mathrm{C} = \frac{iT_{\mathsf{D}}R_{\mathsf{D}}}{\mathrm{Det}}[e^{2i\beta'} - R_{\mathsf{FP}}(0)e^{2i\theta'}]\mathrm{F}_0, \tag{A6b}$$

$$\mathrm{D} = -\frac{iT_{\mathsf{D}}R_{\mathsf{D}}}{\mathrm{Det}}[e^{i(2\beta'+2\theta''-\phi)} - R_{\mathsf{FP}}(0)e^{i(2\theta-\phi)}]\mathrm{F}_0, \tag{A6c}$$

$$\mathrm{E} = -\frac{1}{\mathrm{Det}} \times [R_{\mathsf{D}}^2 e^{2i\beta'} + R_{\mathsf{FP}}(0) \times (T_{\mathsf{D}}^2 + e^{i(2\beta'+2\theta''-\phi)})e^{2i\theta'}]\mathrm{F}_0, \tag{A6d}$$

where

$$\mathrm{Det} = 1 + T_{\mathsf{D}}^2 e^{i(2\beta'+2\theta''-\phi)} + R_{\mathsf{FP}}(0)R_{\mathsf{D}}^2 e^{i(2\theta-\phi)}. \tag{A6e}$$

Suppose then that cavities CI are tuned in resonance and cavities CP are tuned in antiresonance:

$$e^{i(2\theta-\phi)} = -1 \Leftrightarrow 2\theta = (\phi + \pi)\,\mathrm{mod}2\pi, \tag{A7a}$$
$$e^{i(2\beta'+2\theta''-\phi)} = 1 \Leftrightarrow 2\beta' = (-2\theta'' + \phi)\,\mathrm{mod}2\pi = (2\theta' + \pi)2\pi. \tag{A7b}$$

In this case,

$$\mathrm{A} = \frac{iT_{\mathsf{D}}\gamma}{\gamma_{\mathrm{loss}} + T_{\mathsf{D}}^2\gamma_{\mathrm{load}}}\mathrm{F}_0, \tag{A8a}$$
$$\mathrm{C} = -\frac{iR_{\mathsf{D}}T_{\mathsf{D}}\gamma_{\mathrm{load}}}{\gamma_{\mathrm{loss}} + T_{\mathsf{D}}^2\gamma_{\mathrm{load}}}\mathrm{F}_0 e^{2i\theta'}, \tag{A8b}$$
$$\mathrm{D} = -\frac{iR_{\mathsf{D}}T_{\mathsf{D}}\gamma_{\mathrm{load}}}{\gamma_{\mathrm{loss}} + T_{\mathsf{D}}^2\gamma_{\mathrm{load}}}\mathrm{F}_0, \tag{A8c}$$
$$\mathrm{E} = \frac{\gamma_{\mathrm{loss}} - T_{\mathsf{D}}^2\gamma_{\mathrm{load}}}{\gamma_{\mathrm{loss}} + T_{\mathsf{D}}^2\gamma_{\mathrm{load}}}\mathrm{F}_0, \tag{A8d}$$

If $T_{\mathsf{D}} \ll 1$, then the maximum value of the amplitudes A, B is reached when

$$T_{\mathsf{D}} = \frac{\gamma_{\mathrm{loss}}}{\gamma_{\mathrm{load}}}. \tag{A9}$$

In this case (we add here Eq. (A4i) for convenience):

$$\mathrm{A} = \frac{i\gamma}{2\sqrt{\gamma_{\mathrm{load}}\gamma_{\mathrm{loss}}}}\mathrm{F}_0, \tag{A10a}$$

$$\mathrm{C} = -\frac{iR_{\mathrm{D}}}{2}\sqrt{\frac{\gamma_{\mathrm{load}}}{\gamma_{\mathrm{loss}}}}\mathrm{F}_0 e^{2i\theta'} = -R_{\mathrm{D}}\frac{\gamma_{\mathrm{load}}}{\gamma}\mathrm{A}e^{2i\theta'}, \tag{A10b}$$

$$\mathrm{D} = -\frac{iR_{\mathrm{D}}}{2}\sqrt{\frac{\gamma_{\mathrm{load}}}{\gamma_{\mathrm{loss}}}}\mathrm{F}_0 = -R_{\mathrm{D}}\frac{\gamma_{\mathrm{load}}}{\gamma}\mathrm{A}, \tag{A10c}$$

$$\mathrm{E} = 0 \quad \text{(there is no reflected wave)}, \tag{A10d}$$

$$\mathrm{I} = \frac{i\sqrt{c\gamma_{\mathrm{load}}/L}}{\gamma}\mathrm{A}e^{i\theta'}. \tag{A10e}$$

3. Signal mode

The first-order equations are the following (see papers [22,23]):

$$\hat{a}_{1,2}(\omega) = -R_{\mathsf{D}}\hat{d}_{1,2}(\omega) + iT_{\mathsf{D}}\hat{f}_{1,2}(\omega), \tag{A11a}$$

$$\hat{\mathrm{b}}_{1,2}(\omega) = R_{\mathsf{FP}}(\Omega)\hat{\mathrm{a}}_{1,2}(\omega)e^{2i\theta'} + \hat{\mathrm{b}}_{01,02}(\omega), \tag{A11b}$$

$$\hat{\mathrm{c}}_{1,2}(\omega) = -R_{\mathsf{D}}\hat{\mathrm{b}}_{1,2}(\omega) + iT_{\mathsf{D}}\hat{\mathrm{h}}_{1,2}(\omega), \tag{A11c}$$

$$\hat{\mathrm{d}}_{1,2}(\omega) = [-R_{\mathsf{C}}\hat{\mathrm{c}}_{1,2}(\omega) + iT_{\mathsf{C}}\hat{\mathrm{c}}_{2,1}(\omega)]e^{2i\theta''} + \hat{\mathrm{d}}_{01,02}(\omega), \tag{A11d}$$

$$\hat{\mathrm{e}}_{1,2}(\omega) = -R_{\mathsf{D}}\hat{\mathrm{h}}_{1,2}(\omega) + iT_{\mathsf{D}}\hat{\mathrm{b}}_{1,2}(\omega), \tag{A11e}$$

$$\hat{\mathrm{f}}_{1,2}(\omega) = \pm\frac{\hat{\mathrm{e}}_1(\omega) - \hat{\mathrm{e}}_2(\omega)}{2}e^{2i\beta''} + \hat{\mathrm{f}}_0, \tag{A11f}$$

$$\hat{\mathrm{g}}_{1,2}(\omega) = -R_{\mathrm{A}}\hat{\mathrm{f}}_{1,2}(\omega) + iT_{\mathsf{D}}\hat{\mathrm{d}}_{1,2}(\omega), \tag{A11g}$$

$$\hat{\mathrm{h}}_{1,2}(\omega) = -\hat{\mathrm{g}}_{1,2}(\omega)e^{2i\beta'}, \tag{A11h}$$

$$\hat{\mathrm{i}}_{1,2}(\omega) = \frac{i\sqrt{\gamma_{\mathrm{load}}/\tau}}{\gamma - i\Omega}[\hat{\mathrm{a}}_{1,2}(\omega)e^{i\theta'} + \hat{\mathrm{s}}_{1,2}(\omega)], \tag{A11i}$$

where

$$\Omega = \omega - \omega_o, \tag{A12a}$$

$$\hat{\mathrm{b}}_{01,02}(\omega) = \frac{2\gamma_{\mathrm{load}}}{\gamma - i\Omega}\hat{\mathrm{s}}_{1,2}(\Omega)e^{i\theta'}, \tag{A12b}$$

$$\hat{\mathrm{d}}_{01,02}(\omega) = \pm\frac{2i\omega_o \mathrm{C}_{1,2}R_{\mathsf{C}}}{c}\hat{y}(\Omega)e^{2i\theta''}, \tag{A12c}$$

$$\hat{\mathrm{s}}_{1,2}(\omega) = -\sqrt{\frac{\gamma_{\mathrm{loss}}}{\gamma_{\mathrm{load}}}}\hat{\mathrm{n}}_{1,2}(\omega) + \frac{\omega_o \mathrm{I}_{1,2}}{\sqrt{c\gamma_{\mathrm{load}}L}}\hat{x}_{1,2}(\Omega), \tag{A12d}$$

$$\hat{x}_{1,2}(\Omega) = \hat{x}_{\mathsf{E}1,2}(\Omega) - \hat{x}_{\mathrm{l}1,2}(\Omega), \tag{A12e}$$

$\hat{\mathrm{n}}_{1,2}(\omega)$ are the noises created by the internal losses in the Fabry-Perot cavities normalized as zero-point fluctuations and

$$R_{\mathsf{FP}}(\Omega) = \frac{\gamma_- + i\Omega}{\gamma - i\Omega} \tag{A12f}$$

is the arm cavities reflection factor at the (side-band) frequency Ω.

Introduce the antisymmetric mode:

$$\hat{\mathrm{a}}(\omega) = \frac{\hat{\mathrm{a}}_1(\omega) - \hat{\mathrm{a}}_2(\omega)}{\sqrt{2}}, \tag{A13}$$

and correspondingly for all other field amplitudes. Taking into account that

$$\mathrm{C}_1 = \mathrm{C}_2 = \frac{\mathrm{C}}{\sqrt{2}}, \qquad \mathrm{I}_1 = \mathrm{I}_2 = \frac{\mathrm{I}}{\sqrt{2}}, \tag{A14}$$

we obtain the following equations for this mode field amplitudes:

$$\hat{a}(\omega) = -R_{\mathsf{D}}\hat{d}(\omega) + iT_{\mathsf{D}}\hat{f}(\omega), \tag{A15a}$$

$$\hat{\mathrm{b}}(\omega) = R_{\mathsf{FP}}(\Omega)\hat{\mathrm{a}}(\omega)e^{2i\theta'} + \hat{\mathrm{b}}_0(\omega), \tag{A15b}$$

$$\hat{\mathrm{c}}(\omega) = -R_{\mathsf{D}}\hat{\mathrm{b}}(\omega) + iT_{\mathsf{D}}\hat{\mathrm{h}}(\omega), \tag{A15c}$$

$$\hat{\mathrm{d}}(\omega) = -\hat{\mathrm{c}}(\omega)e^{i(2\theta''+\phi)} + \hat{\mathrm{d}}_0(\omega), \tag{A15d}$$

$$\hat{\mathrm{e}}(\omega) = -R_{\mathsf{D}}\hat{\mathrm{h}}(\omega) + iT_{\mathsf{D}}\hat{\mathrm{b}}(\omega), \tag{A15e}$$

$$\hat{\mathrm{f}}(\omega) = \hat{\mathrm{e}}(\omega)e^{2i\beta''}, \tag{A15f}$$

$$\hat{\mathrm{g}}(\omega) = -R_{\mathrm{A}}\hat{\mathrm{f}}(\omega) + iT_{\mathsf{D}}\hat{\mathrm{d}}(\omega), \tag{A15g}$$

$$\hat{\mathrm{h}}(\omega) = -\hat{\mathrm{g}}(\omega)e^{2i\beta'}, \tag{A15h}$$

$$\hat{\mathrm{i}}(\omega) = \frac{i\sqrt{c\gamma_{\mathrm{load}}/L}}{\gamma - i\Omega}[\hat{\mathrm{a}}(\omega)e^{i\theta'} + \hat{\mathrm{s}}(\omega)], \tag{A15i}$$

where

$$\hat{b}_0(\omega) = \frac{2\gamma_{\mathrm{load}}}{\gamma - i\Omega}\hat{\mathrm{s}}(\Omega)e^{i\theta'}, \tag{A16a}$$

$$\hat{\mathrm{d}}_0(\omega) = \frac{2i\omega_o \mathrm{C}R_{\mathsf{C}}}{c}\hat{y}(\Omega)e^{2i\theta''}, \tag{A16b}$$

$$\hat{\mathrm{s}}(\omega) = -\sqrt{\frac{\gamma_{\mathrm{loss}}}{\gamma_{\mathrm{load}}}}\hat{\mathrm{n}}(\omega) + \frac{i\omega_o \mathrm{A}}{c\gamma L}\hat{x}(\Omega)e^{i\theta'}, \tag{A16c}$$

$$\hat{x}(\Omega) = \frac{\hat{x}_1(\Omega) - \hat{x}_2(\Omega)}{2}. \tag{A16d}$$

Solution of these equations is the following:

$$\det(\Omega)\hat{a}(\omega) = -[R_{\mathsf{D}}^2 e^{i(2\theta''+\phi)} + T_{\mathsf{D}}^2 e^{2i\beta''} + e^{i(2\beta+2\theta''+\phi)}] \times \hat{b}_0(\omega) - R_{\mathsf{D}}(1 + e^{2i\beta})\hat{d}_0(\omega), \tag{A17a}$$

$$\det(\Omega)\hat{\mathrm{c}}(\omega) = -R_{\mathsf{D}}(1 + e^{2i\beta})\hat{\mathrm{b}}_0(\omega) + [R_{\mathsf{FP}}(\Omega) \times (R_{\mathsf{D}}^2 + e^{2i\beta})e^{2i\theta'} + T_{\mathsf{D}}^2 e^{2i\beta'}]\hat{\mathrm{d}}_0(\omega), \tag{A17b}$$

$$\det(\Omega)\hat{\mathrm{d}}(\omega) = R_{\mathsf{D}}e^{i(2\theta''+\phi)}(1 + e^{2i\beta})\hat{\mathrm{b}}_0(\omega) + [1 + R_{\mathsf{D}}^2 e^{2i\beta} \times + R_{\mathsf{FP}}(\Omega)T_{\mathsf{D}}^2 e^{2i(\beta''+\theta')}]\hat{\mathrm{d}}_0(\omega), \tag{A17c}$$

where

$$\det(\Omega) = 1 + R_{\mathsf{D}}^2 e^{2i\beta} + T_{\mathsf{D}}^2 e^{i(2\beta'+2\theta''+\phi)} + R_{\mathsf{FP}}(\Omega) \times [R_{\mathsf{D}}^2 e^{i(2\theta+\phi)} + T_{\mathsf{D}}^2 e^{2i(\beta''+\theta')} + e^{i(2\beta+2\theta+\phi)}]. \tag{A17d}$$

Now conditions Eqs. (A7) and, in addition, the dark port condition for the D–P cavities

$$e^{i(2\theta''+\phi)} = e^{2i\beta''} \Leftrightarrow 2\beta'' = 2\theta' + \phi 2\pi = -2\theta' + 2\phi + \pi 2\pi \tag{A18}$$

are fulfilled. In this case,

$$\det(\Omega) = [1 + e^{2i\phi}][1 - R_{\mathsf{FP}}(\Omega)e^{2i\phi}], \tag{A19}$$

and

$$\hat{c}(\omega) = \frac{-R_{\mathsf{D}}\hat{b}_0(\omega) + R_{\mathsf{D}}^2 R_{\mathsf{FP}}(\Omega)\hat{d}_0(\omega)e^{2i\theta'}}{1 - R_{\mathsf{FP}}(\Omega)e^{2i\phi}} - \frac{T_{\mathsf{D}}^2\hat{d}_0(\omega)e^{2i\theta'}}{1 + e^{2i\phi}}, \tag{A20a}$$

$$\hat{d}(\omega) = \frac{-R_{\mathsf{D}}\hat{b}_0(\omega)e^{2i(-\theta'+\phi)} + R_{\mathsf{D}}^2\hat{d}_0(\omega)}{1 - R_{\mathsf{FP}}(\Omega)e^{2i\phi}} + \frac{T_{\mathsf{D}}^2\hat{d}_0(\omega)}{1 + e^{2i\phi}}, \tag{A20b}$$

$$\hat{i}(\omega) = \frac{i\sqrt{c\gamma_{\mathrm{load}}/L}}{\gamma - i\Omega}\frac{[1 + e^{2i\phi}]\hat{s}(\omega) - R_{\mathsf{D}}\hat{d}_0(\omega)e^{i\theta'}}{1 - R_{\mathsf{FP}}(\Omega)e^{2i\phi}}. \tag{A20c}$$

4. Pondermotive forces

a. Central mirror

Force acting on the central mirror is equal to (taking into account that $\Omega \ll \omega_o$):

$$\begin{aligned}\hat{F}_y(t) &= \frac{\hbar\omega_o}{c}[|C_2|^2 + |D_2|^2 - |C_2|^2 - |D_2|^2] \\ &+ \frac{\hbar\omega_o}{c}\left\{\int_0^\infty [C_2^*\hat{c}_2(\omega) + D_2^*\hat{d}_2(\omega) - C_1^*\hat{c}_2(\omega) \right. \\ &\left. - D_1^*\hat{d}_1(\omega)] \times e^{i(\omega_o-\omega)t}\frac{d\omega}{2\pi} + \text{h.c.}\right\} \\ &= -\hbar\int_0^\infty \kappa(\omega)[C^*\hat{c}(\omega) + D^*\hat{d}(\omega)]e^{i(\omega_o-\omega)t}\frac{d\omega}{2\pi} \\ &+ \text{h.c.},\end{aligned} \tag{A21}$$

where h.c. stands for "Hermitian conjugate."

In the spectral domain this equation has the following form:

$$\hat{F}_y(\Omega) = \hat{\mathcal{F}}_y(\Omega) + \hat{\mathcal{F}}_y^+(-\Omega), \tag{A22}$$

where

$$\hat{\mathcal{F}}_y(\Omega) = -\frac{\hbar\omega_o}{c}[C^*\hat{c}(\omega_o + \Omega) + D^*\hat{d}(\omega_o + \Omega)]. \tag{A23}$$

Substituting here field amplitudes (A10) and (A 3) we obtain:

$$\begin{aligned}\hat{\mathcal{F}}_y(\Omega) &= \frac{\hbar\omega_o C^* R_{\mathsf{D}}}{c[1 - R_{\mathsf{FP}}(\Omega)e^{2i\phi}]}[(1 + e^{2i\phi})\hat{b}_0(\omega) \\ &- R_{\mathsf{D}}[1 + R_{\mathsf{FP}}(\Omega)]\hat{d}_0(\omega)e^{2i\theta'}] \\ &= \hat{\mathcal{F}}_{y\mathrm{loss}}(\Omega) + \mathcal{K}_{yx}(\Omega)\hat{x}(\Omega) - \mathcal{K}_{yy}(\Omega)\hat{y}(\Omega),\end{aligned} \tag{A24}$$

where

$$\hat{\mathcal{F}}_{y\,\mathrm{loss}}(\Omega) = \frac{2\hbar\omega_o C^* R_{\mathrm{D}}\sqrt{\gamma_{\mathrm{load}}\gamma_{\mathrm{loss}}}}{ic(\Omega_B + i\gamma_{\mathrm{loss}} + \Omega)}\hat{n}(\omega)e^{i\theta'}, \tag{A25a}$$

$$\mathcal{K}_{yy}(\Omega) = \frac{2\hbar\omega_o^2|C|^2 R_{\mathsf{D}}^2\gamma_{\mathrm{load}}}{c^2(\Omega_B + i\gamma_{\mathrm{loss}} + \Omega)}, \tag{A25b}$$

$$\mathcal{K}_{yx}(\Omega) = \frac{2\hbar\omega_o^2|AC|R_{\mathsf{D}}\gamma_{\mathrm{load}}}{c\gamma L(\Omega_B + i\gamma_{\mathrm{loss}} + \Omega)}, \tag{A25c}$$

and

$$\Omega_B = \gamma_{\mathrm{load}}\tan\phi. \tag{A26}$$

It should be noted that Eq. (A26) is valid only if

$$\gamma_{\mathrm{load}}\tan\phi \ll c/L; \tag{A27}$$

more precise formula is the following:

$$\Omega_B = \frac{c}{L}\arctan\left(\frac{\gamma_{\mathrm{load}}L}{c}\tan\phi\right), \tag{A28}$$

see [28].

b. Arm cavities

Forces which act on the mirrors I, E are equal to (see papers [22,23]):

$$\begin{aligned}\hat{F}_{x1,2}(\Omega) &= -\hat{F}_{\mathsf{I}1,2}(\Omega) = \hat{F}_{\mathsf{E}1,2}(\Omega) \\ &= \hat{\mathcal{F}}_{x1,2}(\Omega) + \hat{\mathcal{F}}_{x1,2}^+(-\Omega),\end{aligned} \tag{A29}$$

where

$$\hat{\mathcal{F}}_{x1,2}(\Omega) = \frac{2\hbar\omega_o I_{1,2}^*\hat{i}_{1,2}(\omega)}{c}. \tag{A30}$$

Introduce differential force:

$$\hat{F}_x(\Omega) = \hat{F}_{x1}(\Omega) - \hat{F}_{x2}(\Omega) = \hat{\mathcal{F}}_x(\Omega) + \hat{\mathcal{F}}_x^+(-\Omega). \tag{A31}$$

For this force we obtain:

$$\begin{aligned}\hat{\mathcal{F}}_x(\Omega) &= \hat{\mathcal{F}}_{x1}(\Omega) - \hat{\mathcal{F}}_{x2}(\Omega) \\ &= \hat{\mathcal{F}}_{x\mathrm{fl}}(\Omega) - \mathcal{K}_{xx}(\Omega)\hat{x}(\Omega) + \mathcal{K}_{xy}(\Omega)\hat{y}(\Omega),\end{aligned} \tag{A32}$$

where

$$\hat{\mathcal{F}}_{x\mathrm{loss}}(\Omega) = -F\hat{\mathcal{F}}_{y\mathrm{loss}}(\Omega), \tag{A33a}$$

$$\mathcal{K}_{xy}(\Omega) = \frac{2\hbar\omega_o^2|\mathrm{AC}|R_{\mathrm{D}}\gamma_{\mathrm{load}}}{c\gamma L(\Omega_B + i\gamma_{\mathrm{loss}} + \Omega)}, \tag{A33b}$$

$$\mathcal{K}_{xx}(\Omega) = \frac{2\hbar\omega_o^2|\mathrm{A}|^2\gamma_{\mathrm{load}}}{(\gamma L)^2(\Omega_B + i\gamma_{\mathrm{loss}} + \Omega)}. \tag{A33c}$$

5. Mechanical equations of motion

It is easy to note that

$$\hat{\mathcal{F}}_{x\mathrm{loss}}(\Omega) = -F\hat{\mathcal{F}}_{y\mathrm{loss}}(\Omega), \tag{A34a}$$

$$\mathcal{K}_{xx}(\Omega) = F\mathcal{K}_{xy}(\Omega) = F\mathcal{K}_{yx}(\Omega) = F^2\mathcal{K}_{yy}(\Omega). \tag{A34b}$$

where

$$F = \frac{c}{\gamma_{\mathrm{load}}LR_{\mathrm{D}}^2} \gg 1. \tag{A35}$$

Therefore, the fluctuation forces spectral densities and the pondermotive rigidities are described by the following equations:

$$S_{x\mathrm{loss}}(\Omega) = F^2S_{y,\mathrm{loss}}(\Omega) = \frac{8\hbar\omega_o W\gamma_{\mathrm{loss}}}{cL}\frac{\Omega_B^2 + \gamma_{\mathrm{loss}}^2 + \Omega^2}{|\mathcal{D}(\Omega)|^2}, \tag{A36a}$$

$$K_{xx}(\Omega) = K_{xy}(\Omega) = K_{yx}(\Omega) = F^2K_{yy}(\Omega) = \frac{8\omega_o W}{cL}\frac{\Omega_B}{\mathcal{D}(\Omega)}, \tag{A36b}$$

where

$$\mathcal{D}(\Omega) = (-i\Omega + \gamma_{\mathrm{loss}})^2 + \Omega_B^2, \tag{A37}$$

and

$$W = \hbar\omega_o|\mathrm{I}_{1,2}|^2 = \frac{\hbar\omega_o|\mathrm{I}|^2}{2} \tag{A38}$$

is the optical power circulating in the arm cavities.

The "raw" set of the mechanical equations for all five test masses is the following:

$$M_{\mathrm{l}}\frac{d^2\hat{x}_{\mathrm{l}1,2}(t)}{dt^2} = -\hat{F}_{x1,2}(t), \tag{A39a}$$

$$M_{\mathrm{E}}\frac{d^2\hat{x}_{\mathrm{E}1,2}(t)}{dt^2} = \hat{F}_{x1,2}(t) \pm M_{\mathrm{E}}a_{\mathrm{sign}}(t), \tag{A39b}$$

$$M_{\mathrm{C}}\frac{d^2\hat{y}(t)}{dt^2} = \hat{F}_y(t) + \hat{F}_{\mathrm{meter}}(t), \tag{A39c}$$

where

$$a_{\mathrm{sign}}(t) = \frac{L\ddot{h}(t)}{2} \tag{A40}$$

is the signal acceleration, $h(t)$ is the gravitational-wave signal and $\hat{F}_{\mathrm{meter}}$ is the meter backaction force.

Excluding mechanical degrees of freedom not coupled with the local mirror these five equations can be reduced to the following two ones:

$$M\frac{d^2\hat{x}(t)}{dt^2} = \hat{F}_x(t) + Ma_{\mathrm{sign}}(t), \tag{A41a}$$

$$M_{\mathrm{C}}\frac{d^2\hat{y}(t)}{dt^2} = \hat{F}_y(t) + \hat{F}_{\mathrm{meter}}(t). \tag{A41b}$$

Insert here pondermotive forces calculated in the previous subsubsection and rewrite the equations in spectral representation:

$$[-M\Omega^2 + K_{xx}(\Omega)]\hat{x}(\Omega) = K_{xy}(\Omega)\hat{y}(\Omega) + \hat{F}_{x\mathrm{loss}}(\Omega) + Ma_{\mathrm{sign}}(\Omega), \tag{A42a}$$

$$[-M_{\mathrm{C}}\Omega^2 + K_{yy}(\Omega)]\hat{y}(\Omega) = K_{yx}(\Omega)\hat{x}(\Omega) + \hat{F}_{y\mathrm{loss}}(\Omega) + \hat{F}_{\mathrm{meter}}(\Omega). \tag{A42b}$$

Taking into account symmetry conditions (A34) we obtain:

$$-m_+\Omega^2[-m_*\Omega^2 + K_{yy}(\Omega)]\hat{y}(\Omega) = \mu K_{yy}(\Omega)Fa_{\mathrm{sign}}(\Omega) - \mu\Omega^2\hat{F}_{y\mathrm{loss}}(\Omega) + [-\mu\Omega^2 + K_{yy}(\Omega)]\hat{F}_{\mathrm{meter}}(\Omega). \tag{A43}$$

The ratio of the first two terms in the right-hand part of this equation defines the sensitivity limitation imposed by optical losses. Spectral density of the corresponding equivalent noise (normalized as fluctuation metrics variation) is equal to

$$S_h^{\mathrm{loss}}(\Omega) = \frac{4}{L^2\Omega^4}\frac{\Omega^4S_y^{\mathrm{loss}}(\Omega)}{F^2L^2|K_{yy}(\Omega)|^2} = \frac{\hbar c\gamma_{\mathrm{loss}}}{2\omega_o WL}\frac{\Omega_B^2 + \gamma_{\mathrm{loss}}^2 + \Omega^2}{\Omega_B^2}. \tag{A44}$$

In the next section analyzing the local meter schemes we will neglect optical losses both in the main (large) scheme and in the local meter. In this case Eq. (A43) can be simplified:

$$D(i\Omega)\hat{y}(\Omega) = \mu\Omega_B^2\Omega_0^2Fa_{\mathrm{sign}}(\Omega) + D_F(i\Omega)\hat{F}_{\mathrm{meter}}(\Omega), \tag{A45}$$

where

$$D(s) = m_+s^2(s^4 + \Omega_B^2s^2 + \Omega_B^2\Omega_0^2), \tag{A46a}$$

$$D_F(s) = \frac{\mu}{m_*}s^2(s^2 + \Omega_B^2) + \Omega_B^2\Omega_0^2, \tag{A46b}$$

$$\Omega_0^2 = \frac{K_{yy}(0)}{m_*} = \frac{8\omega_o W}{F^2m_*cL\Omega_B}. \tag{A47}$$

APPENDIX B: ANALYSIS OF THE LOCAL METER

1. Ideal variation measurement

The output signal of the meter which monitors the local mirror position y, can be presented as the following [see Eq. (A45)]:

$$\tilde{y}(\Omega) = \hat{y}(\Omega) + \hat{y}_{\rm meter}(\Omega) = \frac{\mu\Omega_0^2\Omega_B^2 F}{D(i\Omega)}[a_{\rm sign}(\Omega) + \hat{a}_{\rm fluct}(\Omega)], \tag{B1}$$

where

$$\hat{a}_{\rm fluct}(\Omega) = \frac{D(i\Omega)\hat{y}_{\rm meter}(\Omega) + D_F(i\Omega)\hat{F}_{\rm meter}(\Omega)}{\mu\Omega_0^2\Omega_B^2 F}, \tag{B2}$$

and $\hat{y}_{\rm meter}$, and $\hat{F}_{\rm meter}$ are meter noises. If the meter cavity is sufficiently short then these noises spectral densities are equal to:

$$S_y = \frac{S_0}{\sin^2\phi_{\rm LO}}, \qquad S_F = \frac{\hbar^2}{4S_0}, \qquad S_{yF} = \frac{\hbar}{2}\cot\phi_{\rm LO}, \tag{B3}$$

and

$$S_0 = \frac{\hbar c^2 T_{\rm local}^2}{64\omega_o w} \tag{B4}$$

is the *residual* noise of the variation meter.

Spectral density of noise $\hat{a}_{\rm fluct}(\Omega)$ is equal to:

$$S_a^{\rm meter} = \frac{1}{(\mu\Omega_0^2\Omega_B^2 F)^2}[D^2(i\Omega)S_y + 2D(i\Omega)D_F(i\Omega)S_{yF} + D_F^2(i\Omega)S_F]. \tag{B5}$$

It reaches minimum if

$$\cot\phi_{\rm LO} = -\frac{\hbar}{2S_0}\frac{D_F(i\Omega)}{D(i\Omega)}, \tag{B6}$$

and this minimum is equal to:

$$S_a^{\rm meter} \equiv \frac{L^2\Omega^4}{4}S_h^{\rm meter} = \frac{D^2(i\Omega)}{(\mu\Omega_0^2\Omega_B^2 F)^2}S_0 = \frac{[\Omega^4 - \Omega^2\Omega_B^2 + \Omega_0^2\Omega_B^2]^2}{\Omega_0^4\Omega_B^4}\frac{m_+^2}{\mu^2}\frac{\Omega^4 S_0}{F^2}. \tag{B7}$$

2. DSVM-based local meter

In the time-domain form the Eq. (A45) can be presented as the following:

$$\mathbf{D}\,\hat{y}(t) = \mu\Omega_B^2\Omega_0^2 F a_{\rm sign}(t) + \mathbf{D}_F\hat{F}_{\rm meter}(t), \tag{B8}$$

where

$$\mathbf{D} = D(d/dt), \qquad \mathbf{D}_F = D_F(d/dt). \tag{B9}$$

The local meter output signal is equal to:

$$\tilde{y}(t) = \hat{y}(t) + \hat{y}_{\rm meter}(t), \tag{B10}$$

where $\hat{y}_{\rm meter}(t)$ is the meter additive noise.

Following the DSVM procedure (see [33]) we suppose that: (i) noises $\hat{y}_{\rm meter}(t)$ and $\hat{F}_{\rm meter}(t)$ correlate with each other:

$$\hat{y}_{\rm meter}(t) = \hat{y}^{(0)}_{\rm meter}(t) + \alpha(t)\hat{F}_{\rm meter}(t), \tag{B11}$$

where $\alpha(t)$ is some given function, and (ii) during a sufficiently short time interval τ the signal $a_{\rm sign}(t)$ can be considered as constant one. Estimate for this constant can be found using the following equation:

$$\tilde{a}_{\rm sign} = \frac{1}{\mu\Omega_B^2\Omega_0^2 F\bar{v}}\int_\tau v(t)\mathbf{D}\tilde{y}(t)dt = a_{\rm sign} + \frac{1}{\mu\Omega_B^2\Omega_0^2 F\bar{v}}\int_\tau v(t)\Big\{\mathbf{D}\hat{y}^{(0)}_{\rm meter}(t) + \left[\mathbf{D}\alpha(t) + \frac{1}{m_+}\mathbf{D}_F\right]\hat{F}_{\rm meter}(t)\Big\}dt, \tag{B12}$$

where $v(t)$ is filter function and

$$\bar{v} = \int_\tau v(t)dt. \tag{B13}$$

For the short local meter cavity the local meter noises can be considered as ''white'' or δ-correlated ones.

The term proportional to the backaction force $\hat{F}_{\rm meter}(t)$ can be canceled by the proper choice of $\alpha(t)$ (and this is the essence of the variation measurement). In this case the measurement error will be equal to:

$$(\Delta a)^2 = \left(\frac{1}{\mu\Omega_B^2\Omega_0^2 F\bar{v}}\right)^2 S_0\int_\tau[\mathbf{D}v(t)]^2 dt, \tag{B14}$$

where S_0 is the residual meter noise $\hat{y}^{(0)}_{\rm meter}(t)$ spectral density, see Eq. (B4).

Therefore, filter function $v(t)$ that provides minimum to the measurement error functional should satisfy the following Lagrange equation:

$$\mathbf{D}^2 v = 1, \tag{B15}$$

with the following boundary conditions

$$v(\pm\tau/2) = 0, \qquad \frac{d^n v(t)}{dt^n}\Big|_{t=\pm\tau/2} = 0 \qquad (n = 1\ldots 5). \tag{B16}$$

Solution of this equation can be represented as the following:

$$v(t) = \frac{t^4}{24m_+^2\Omega_B^4\Omega_0^4} + C_1 t^2 + C_2 + C_3 t\sin\Omega_+ t + C_4\cos\Omega_+ t + C_5 t\sin\Omega_- t + C_6\cos\Omega_- t, \tag{B17}$$

where

$$\Omega_{\pm}^2 = \frac{\Omega_B^2}{2} \pm \sqrt{\frac{\Omega_B^4}{4} - \Omega_B^2 \Omega_0^2}, \tag{B18}$$

and coefficients $\{C_i\}$ can be found from boundary conditions (B16). We do not give the exact formulae for $\{C_i\}$ because they are quite cumbersome and will add to our article several more pages (not very informative ones, we think).

Being substituted to (B14) function υ will give the minimum measurement error:

$$(\Delta a)^2 = \frac{S_0}{(\mu \Omega_B^2 \Omega_0^2 F)^2 \bar{\upsilon}} = \frac{720}{\tau^5} \frac{m_+^2}{\mu^2} \frac{S_y}{F^2} \frac{1}{\mathcal{G}(\Omega_B, \Omega_0)}, \tag{B19}$$

where 3D-plot of the function $\mathcal{G}(\Omega_B, \Omega_0)$ is presented in Fig. 5. It should be noted that function $\mathcal{G}$ is defined only in the area where $\Omega_0 < \Omega_B/2$ and the frequencies $\Omega_{\pm}$ are real and the system is dynamically stable. The exact expression for $\mathcal{G}$ we do not give in this paper due to the same reason as for coefficients $\{C_i\}$.

Sequence of discrete measurements with the measurement error Δa is equivalent to continuous monitoring of the signal acceleration a with the sensitivity defined by the equivalent spectral density

$$S_a^{\text{meter}} \equiv \frac{L^2 \Omega^4}{4} S_h^{\text{meter}} = (\Delta a)^2 \tau = \frac{720}{\pi^4} \frac{m_+^2}{\mu^2} \frac{\Omega_{\max}^4 S_y}{F^2} \frac{1}{\mathcal{G}(\Omega_B, \Omega_0)}. \tag{B20}$$

[1] A. Abramovici *et al.*, Science **256**, 325 (1992).
[2] B. Caron *et al.*, Classical Quantum Gravity **14**, 1461 (1997).
[3] M. Ando *et al.*, Phys. Rev. Lett. **86**, 3950 (2001).
[4] B.Willke *et al.*, Classical Quantum Gravity **19**, 1377 (2002).
[5] Stan Whitcomb, State of the LIGO Lab, 2005, LIGO Document G050124-00-M (www.ligo.caltech.edu/docs/G/G050124-00.pdf).
[6] V. B. Braginsky, Sov. Phys. JETP **26**, 831 (1968).
[7] V. B. Braginsky and F. Ya. Khalili, *Quantum Measurement* (Cambridge University Press, Cambridge, England, 1992).
[8] V. B. Braginsky, M. L.Gorodetsky, F. Ya. Khalili, A. B. Matsko, K. S. Thorne, and S. P.Vyatchanin, Phys. Rev. D **67**, 082001 (2003).
[9] E. Gustafson, D. Shoemaker, K. A. Strain, and R. Weiss, LSC White paper on detector research and development, LIGO Document T990080-00-D, 1999, (www.ligo.caltech.edu/docs/T/T990080-00.pdf).
[10] P. Fritschel, in *Gravitational Wave Detection*, Proc. SPIE Int. Soc. Opt. Eng. Vol. 4856–39 (SPIE-International Society for Optical Engineering, Bellingham, WA, 2002), p. 282.
[11] H. J. Kimble, Yu. Levin, A. B. Matsko, K. S. Thorne, and S. P. Vyatchanin, Phys. Rev. D **65**, 022002 (2002).
[12] A.Buonanno and Y.Chen, Phys. Rev. D **64**, 042006 (2001).
[13] F. Ya. Khalili, Phys. Lett. A **288**, 251 (2001).
[14] A. Buonanno and Y. Chen, Phys. Rev. D **65**, 042001 (2002).
[15] A. Buonanno and Y. Chen, Phys. Rev. D **67**, 062002 (2003).
[16] J. Harms, Y. Chen, S. Chelkowski, A. Franzen, H. Vahlbruch, K. Danzmann, and R. Schnabel, Phys. Rev. D **68**, 042001 (2003).
[17] A. Buonanno and Y. Chen, Phys. Rev. D **69**, 102004 (2004).
[18] V. B. Braginsky, M. L. Gorodetsky, F. Ya. Khalili, and K. S. Thorne, Phys. Rev. D **61**, 044002 (2000).
[19] P. Purdue, Phys. Rev. D **66**, 022001 (2002).
[20] P. Purdue and Y. Chen, Phys. Rev. D **66**, 122004 (2002).
[21] Y. Chen, Phys. Rev. D **67**, 122004 (2003).
[22] F. Ya. Khalili, gr-gc/0211088.
[23] S. L. Danilishin, Phys. Rev. D **69**, 102003 (2004).
[24] V. B.Braginsky, M. L.Gorodetsky, F. Ya. Khalili, and K. S. Thorne, in *Proceedings of the Third Edoardo Amaldi Conference—Gravitational waves, Pasadena, California, 2000*, AIP Conf. Proc. No. 523 edited by S. Meshkov (AIP, Melville, NY, 2000) p. 180–189.
[25] V. B. Braginsky and F. Ya. Khalili, Phys. Lett. A **218**, 167 (1996).
[26] V. B. Braginsky, M. L. Gorodetsky, and F. Ya. Khalili, Phys. Lett. A **232**, 340 (1997).
[27] V. B. Braginsky, M. L. Gorodetsky, and F. Ya. Khalili, Phys. Lett. A **246**, 485 (1998).
[28] F. Ya. Khalili, Phys. Lett. A **298**, 308 (2002).
[29] F. Ya. Khalili, Phys. Lett. A **317**, 169 (2003).
[30] V. B.Braginsky and F. Ya. Khalili, Phys. Lett. A **257**, 241 (1999).
[31] V. B. Braginsky, F. Ya. Khalili, and S. P. Volikov, Phys. Lett. A **287**, 31 (2001).
[32] I. A. Bilenko and A. A. Samoilenko, Vestnik Moscovskogo Universiteta, Series 3, No. 4, 39 (2003) (in Russian).
[33] S. L. Danilishin, F. Ya. Khalili, and S. P. Vyatchanin, Phys. Lett. A **278**, 123 (2000).
[34] T. Corbitt, K. Goda, N. Mavalvala, E. Mikhalov, D. Ottaway, S. Whitcomb, and Y. Chen, Ponderomotive Squeezing, 2004, LIGO Document G040147-00 (www.ligo.caltech.edu/docs/G/G040147-00).
[35] S. P. Vyatchanin and E. A. Zubova, Phys. Lett. A **201**, 269 (1995).
[36] S. P. Vyatchanin and A. B. Matsko, JETP **83**, 690 (1996).
[37] S. P. Vyatchanin, Phys. Lett. A **239**, 201 (1998).